International Journal of Nanomaterials and Chemistry

http://dx.doi.org/10.12785/ijnc/010301

Potential Removal of Crystal violet (CV), Acid Red (AR) and Methyl Orange (MO) from Aqueous Solution by Magnetic Nanoparticles

*Badriah Saad Al-Farhan**.

Department of Chemistry, Faculty of Girls for Science, King Khalid University, Abha, Saudi Arabia, KSA.

Received: 7 Jun. 2015, Revised: 8 Aug. 2015, Accepted: 9 Aug. 2015.
Published online: 1 Sep. 2015.

Abstract: In this paper bentonite coated with mangentic Fe_2O_3 nanoparticle was prepared and characterized by SEM and XRD. The prepared magnetic nanoparticles was used for the removal of anionic dyes, acid red (AR), methyl orange (MO) and crystal violet (CV) from aqueous solutions. The effect of dye solution pH and contact time were studied. According to the obtained results both AR and CV showed maximum removal efficiency at pH 7 while MO at pH 4. The results showed there are high removal efficiency of the magnetic nanoparticles for the removal of the different organic dyes and the removal efficiency had the order CV > AR > MO. The results explained using the FTIR and TG/DTA analysis and were related to the structure of the organic dye and the function groups on it which interact with the magnetic nanoparticles.

Keywords: organic dyes, anionic dyes, iron compounds, magnetic nanoparticles.

1 Introduction

Progress in industrialization in particular textile industries have led to the discharge of unprecedented amount of wastewater containing synthetic dyes, which pollutes the rivers and consequently causes harm to human and other living organisms [Leechart P et al. 2009]. A majority of the used dyes are azo reactive dyes which are bright in color due to the presence of one or several azo (─N═N─) groups associated with substituted aromatic structures [Bhatnagar A and Jain AK, 2005]. These dyes or their breakdown products are toxic to living organisms [Chung KT et al, 1981]. Furthermore, if these dyes are delivered to water sources, considerable amount of colored wastewater is generated. The presence of these dyes in water even at very low concentration is highly visible and undesirable. These dye stuffs are stable to light, heat and oxidizing agents. In short, they are not easily degradable [Jain, R. and Sikarwar S., 2008]. Methyl orange (MO), crystal violet (CV) and acid red (AR) is a commonly used monoazo dye in laboratory assays, textiles and other commercial products and has to be removed from water due to their toxicity [Mittal A et al, 2007, Chen S et al, 2010].

A wide range of methods have been developed for the removal of synthetic dyes from waters and wastewaters to decrease their impact in environment. Among these adsorption [Gupta VK et al, 2004, Mittal A et al, 2005, Oliveira LCQ, 2003, Herrea F et al 2001].

In recent years, nanocomposite materials consisting of core and shell have been attracting great interest and attention of researchers because of their potential application in catalysis, environmental protection, and especially biomedical use. Materials in the nanosized range are considered the best candidates in the removal of organic and inorganic pollutants from the environment because of their unique physicochemical properties and their super adsorption capacities [Tahir S and Rauf N, 2006, Liu Y et al, 2014, Crini G, 2006]. Herrea et al. [Herrea F et al 2001] have studied the effectiveness of hematite fine particles as adsorbent/ catalyst for the adsorption and catalytic combustion of azo-dye, Orange II, and obtained promising results.

Naturally occurring clays are bellowing to low cost materials with good adsorption ability [Li Y and Liu Y, 2013]. This ability comes from their high specific surface area, chemical and mechanical stability, layered structure and high cations exchange capacity (CEC). Bentonite, naturally occurring clay, a cheap and a widespread material have been used as an alternative material for the removal of dyes. The combination between the properties of the natural clays and the unique properties of the nanoparticle can give rise to effective and economic adsorbent [Naimeh A et al, 2013].

This paper presents the test method for the synthesis of magnetic nanoparticle systems, based on a hematite

* Corresponding author E-mail: shahd_bb@hotmail.com

structure. The studies used the colloidal solution of iron hydroxide (III) and iron oxide (II) to prepare Bentonite/ hematite nanoparticles. The efficiency of these nanoparticles for the removal of three different synthetic dyes stuff, namely: acid red, crystal violet and methyl orange was studied. The effect of pH, contact time and initial dye concentration was also evaluated.

2 Experimental Section

2.1. Chemicals and Dyestuffs

Three different commercial available dyestuffs were used in this study. Crystal violet, methyl orange and acid red. All dyestuffs were purchased from Sigma Aldrich and used without further purification. The characteristics of the selected dyestuffs are listed in Table I. FeCl3 and $FeCl_2$ (Aldrich, analytical purity) were used in the preparation of Fe_2O_3 nanoparticles. All other chemicals were all analytical grade and all solutions were prepared with distilled water.

Table (1): the name of anionic dye and their characterization

Dye (C.I.name)	Supplier	λ_{max} (nm)	Purity %	Molecular formula
Acid red138 (AR)	Aldrich	510	60%	$Na_2C_{30}H_{38}N_3O_8S_2$
Crystal violet(CV)	Aldrich	590	63%	$C_{25}H_{30}N_3Cl$
Methyl orange (MO)	Aldrich	465	85%	C14H14N3NaO3S

2.2 Preparation of magnetic nanoparticles

Bentonite/Fe_2O_3 nanoparticles were prepared as follows:

A solution containing iron (II) chloride (0.02 molar) and iron (III) chloride (0.04 molar) was prepared at room temperature. The suspension was slowly acidified with 1 M HCl until the pH = 4-5. 60 ml of 0.35M $Fe(NO_3)_3$ was added and the solution boiled for one hour. 20 g of bentonite clay was introduced to the resulted suspension and the suspension was left to settle down then filtrated. The solid obtained washed with distilled water several times and dried in an oven at 60ºC for 24 hrs.

2.3 Characterization of nanoparticles by XRD and SEM

The structural properties of synthesized nanoparticles were analyzed by X-ray powder diffraction (XRD) with a Philips X'Pert-MPD System. Scanning electron microscope was carried out by using a JEOL JEM2010 scanning electron microscope operated at 40 kV and 25 mA.

2.4 Declaration Experiment

2.4.1 Effect of dye pH

Since the removal of dye is pH dependent the effect of pH of the dye solution was studied (2-10) for 24hrs at 25 °C. These were performed by adding 0.5 g of Bentonite / Fe_2O_3 Nanoparticles into 250 mL Erlenmeyer flasks containing 50 ml solutions of 100 mg/L of different dyes for 24 hrs. At the end of experiment, filtration was carried out and the remaining dye concentrations were determined by using single beam UV/ visible spectrophotometer (Genesys 20 Thermo Spectronic, Krackeler Scientific) at maximum wavelength 590, 510 and 465 nm for crystal violet, acid red and methyl orange respectively. The concept of a relative percentage efficiency coefficient (E) of removing individual dyes was introduced and defined by the equation (1):

$$E = \frac{(A_0 - A_1)}{A_0} \cdot 100\% \quad (1)$$

Where

A_0 – initial absorbance of the test dye solution (before the process of adsorption)

A_1 – absorbance of the test dye solution determined after treatment with nanoparticles.

2.4.2 Effect of contact time

0.5 g of Bentonite/Fe_2O_3 Nanoparticles was agitated into 250 mL Erlenmeyer flasks containing 50 ml solutions of dyes concentration (1000 mg/L). The temperature was controlled at 25°C. Agitation speed was kept constant at 150 rpm for different times intervals to study the equilibrium conditions of different dye. After each time intervals, Filtration was carried out and the remaining concentration of each dye was measured as mention above and the relative percentage efficiency coefficient, E, was calculated using equation (1). The solid residue in the filter paper was dried in an oven for 24 hrs at 60°C and store in a dissector for TG/DTA and FTIR analysis.

3 Results and Discussion

3.1 Structure and Composition of the Materials.

3.1.1 X-ray

Generally, XRD can be used to characterize the phase composition of the used clay and the crystallinity of the prepared nano-particles. Fig.1 shows the XRD patterns of natural bentonite and bentonite loaded with hematite nanoparticles. The XRD pattern of natural bentonite (B sample) shows small peaks of ill-crystalline silicon dioxide (SiO_2) which indicates it is the major constituent of used bentonite. For Bentonite/Fe_2O_3 nanoparticles, XRD patter

shows peaks at 2θ = 26º and 38.7º which are characterized to Fe_2O_3 nano particles. Calculating the grain size according to Debye-Scherrer formula, we obtained 18.16 nm.

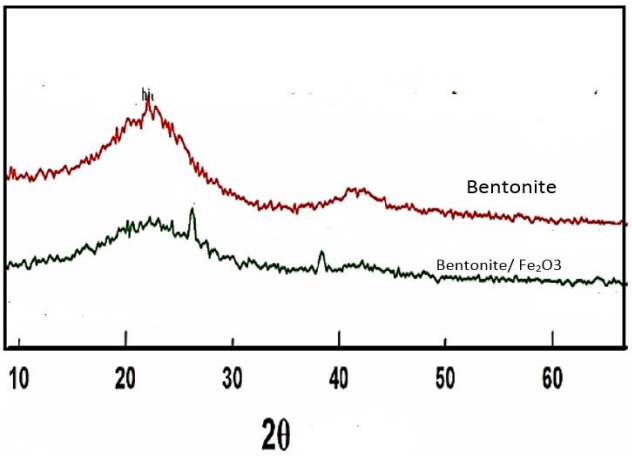

Figure 1: XRD of bentonite and Bentonite/Fe_2O_3 nanoparticles.

3.1.2 Morphology and Shaping of Brntonite/Fe_2O_3 nanoparticles

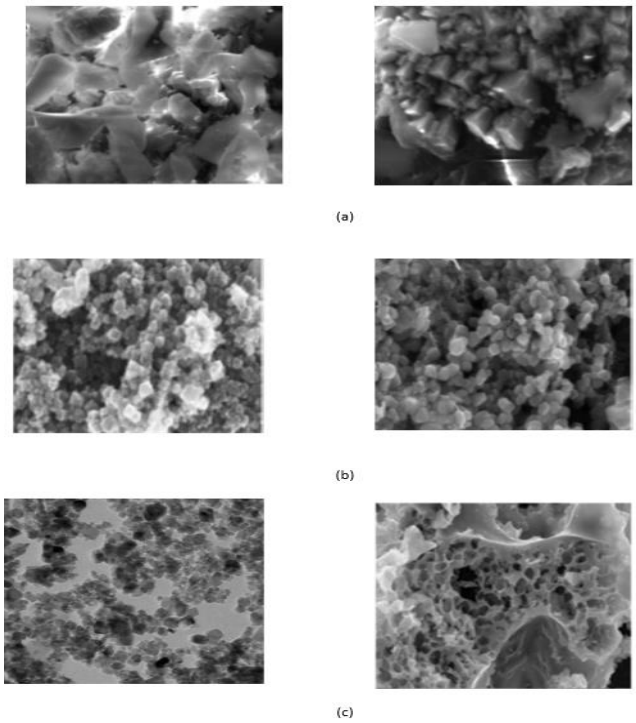

Figure 2: *SEM for (a) bentonite (b) bentonite/ hematite (c) bentonite/magnetite +AR (d) bentonite/magnetite +MO.*

SEM micrographs of natural bentonite and the prepared nanoparticles are shown in Fig.2. Natural bentonite showed platy particles which related to silicon dioxide Fig.2.a. Two types of particles are can be identified from SEM micrographs, the first are of spherical shapes with diameters of 10 nm which are characterized to hematite nanoparticles. These small spherical particles are coated the platy crystals which are characterized to bentonite forming a monalayer on it, Fig 2 b.

When nanoparticle were covered by organic dye, the spherical particle were coved by a colored layer characterized to the molecules of the organic dye. According to the pictures of Fig.2 c,d a single layer of acid red (AR) or methyl orange (MO) was formed on the surface of the nanoparticles.

3.2 Declaration Experiment

3.2.1 Effect of pH on dyes removal

The efficiency of sorption is dependent on the pH of the solution [Aksu Z. and Donmez G, 2003] because variation in pH leads to the variation in the surface properties of the sorbent and the degree of ionization [Gupta V.K et al, 2007]. Thus, comparative experiments were performed over a pH range 2.0 – 10.0 to obtain the optimum pH for adsorption of each dye. The result depicted in Figure 3. For acid red, AR, the dye removal percentage increase in pH range 2-4 and show maximum dye removal in pH range 5-7 then decrease with further increase in pH value. Crystal violet, CV, showed a similar trend of variation of dye removal with pH of the solution with maximum dye removal at pH 7. At low pH value there is a competition between the sorption of the dye molecule and H^+ proton leads to decrease the sorption of the dye on the surface of the nanoparticles. By increasing pH of the solution to become in neutral value, this competition deceased due to decrease in the concentration of H^+ protons by the added base which leads to increase in the dye adsorption and in sequence the dye removal. At higher pH values to become in greater than 7, the concentration of OH^- ions increase which covered the surface of the nanoparticles with a negatively charge. This decreases the adsorption of anionic dyes on it.

For methyl orange (MO), the dye removal is increased from initial pH range = 2 - 4 and then decreased over pH range 5-10, see Fig. 3. This is attributed to the protonation of the surface of the nanoparticles at low pH values. H^+ ions provide a significantly strong electrostatic attraction between the adsorbent surface and the dye molecules leading to maximum adsorption. However, at pH above 4, the degree of protonation of the surface of the nanoparticles will be less which results in the decrease in diffusion and adsorption of the dye molecule due to electrostatic repulsion [Khattri S.D.and Singh M.K, 2009, Baztias F.A. and Sidiras D.K, 2006]. The lower adsorption of the direct dyes in alkaline medium can also be attributed to the competition from hydroxide ions (OH^-) with the anionic dye molecules for the

adsorption sites.

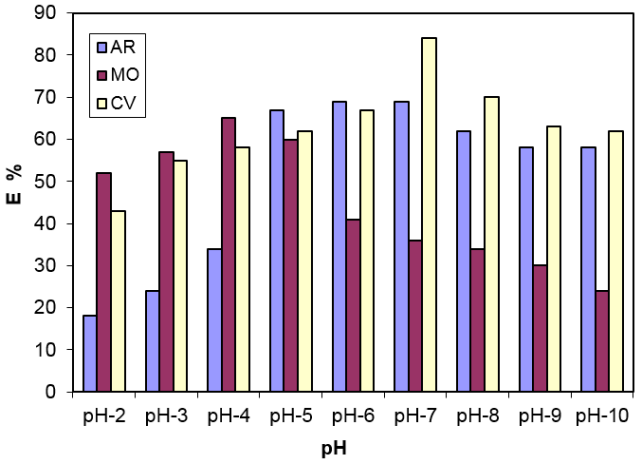

Figure 3: change of percentage of efficiency coefficient (E) with pH of various dyes solutions.

3.2.2 Effect of contact time

The effect of contact time on the percentage removal of different organic dyes was investigated at initial dye concentrations 1000 mg/L was shown in Fig. 4.

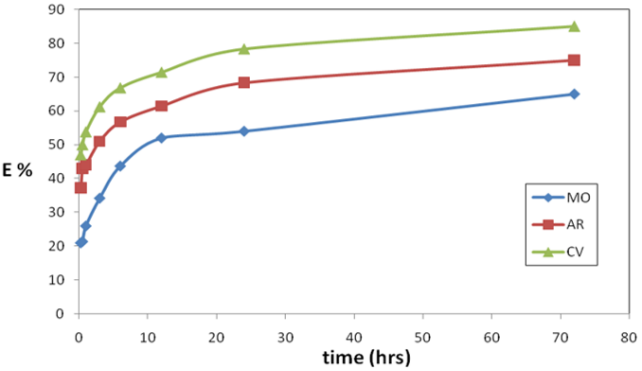

Figure 4: change of percentage of efficiency coefficient (E) with contact time of various dyes solutions.

The pH of the dye solution was kept at constant value for each dye (4 for MO and 7 for CV and AR) represent the pH of the maximum dye removal. In general, for all the dyes studied the removal efficiency increases with increasing the contact time up to 72hrs. The removal was fast in the first 6 hrs which followed by gradual increase in during 6-12 hrs. From 12-72 hrs an equilibrium state was established and no further removal was occurred. However, about 50% of the dye removal was removed during the first two hours indicating a fast equilibrium states were established between the organic dyes and the nanoparticles. From Fig. 4 we can concluded that, the efficiency of Fe_2O_3 for removal of organic dyes had the order CV > AR > MO. This order can be attributed to the structure of the organic dye and the function group on it.

3.2.3 DTA /TG of adsorbed nanoparticles

Figure 5 shows the TGA/DTA curves of solid residue derivatives from soaking of 1000 mg/L of AC with Fe_2O_3 nanoparticle for 24 hrs.

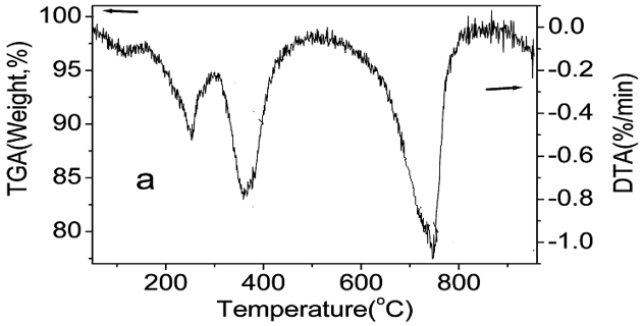

Figure 5: DTA/TG of Bentonite/hematite /acid red after 24 hrs.

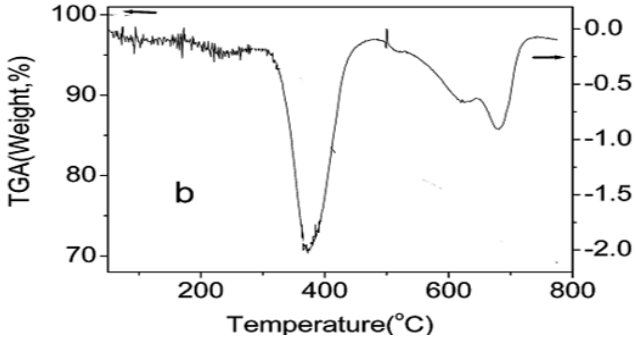

Figure 6: DTA/TG of of Bentonite/hematite /methyl orange after 24 hrs.

There are four derivative peaks in the DTA curve which corresponding to the four mass losses in the TGA curve. The first peak is at about 118ºC, and the percentage mass loss is about 1%, which probably due to the removal of surface adsorbed organic dye. The second peak is at about 250ºC and the percentage of mass loss is about 5%, which probably due to the removal of free AR molecules from the surface of nanoparticles. The position of third peak is at about 397ºC, and the percentage of mass loss is about 8 %, which corresponds to the AR molecules that bind directly with Fe_2O_3 nanoparticle. The mass loss, as well as the high adsorption temperature, confirms strong binding between the AR molecules and Fe_2O_3 nanoparticle. The fourth peak is a broad band at 780 ºC, and the percentage of mass loss is about 7.2%, which is due to the phase transition from Fe_2O_3 to FeO, because FeO is thermodynamically stable above 570 ºC in phase diagram of the Fe-O system

DTA /TG of solid residue derivatives from soaking of 1000 mg/L of MO with Fe_2O_3 nanoparticle for 24 hrs is shown in Fig. 6 . The main notice here is the disappearance of the first peak which found in Figure 5 at 118 ºC. This indicates that MO molecules removed from the dye solution bind only to nanoparticles and there is no free MO molecules on the surface of the nano particles. In Fig. 6 there are two peaks

are appeared in DTA curve corresponding to two stages of weight loss in TGA curve. The first peak was at 380°C with a percentage mass loss about 12 % which can be deduced to the MO directly bind to Fe_2O_3 nanoparticle. The second peak which consists of two collapsed peaks appeared at 690°C with a total percentage mass loss 4.8%. Such peak corresponding to phase transition of Fe_2O_3 to FeO. This indicates that MO molecules removed from the dye solution bind only to nanoparticles and there is no free MO on the surface.

3.2.4 FTIR

FTIR has often been used as a useful tool in determining specific functional groups or chemical bonds that exist in a material. The presence of a peak at a specific wave number would indicate the presence of a specific chemical bond. Fig.7a,b illustrates the FT-IR spectra of Bentonite/hematite soaked in MO dye solution for 3 and 24 hrs respectively.

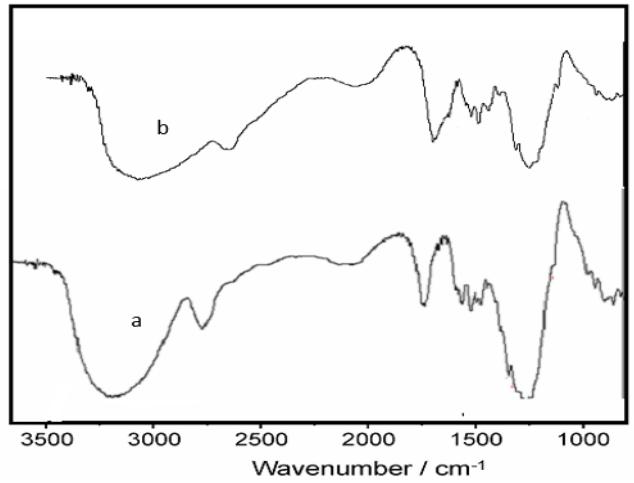

Figure 7: FTIR of of Bentonite/hematite /methyl orange.

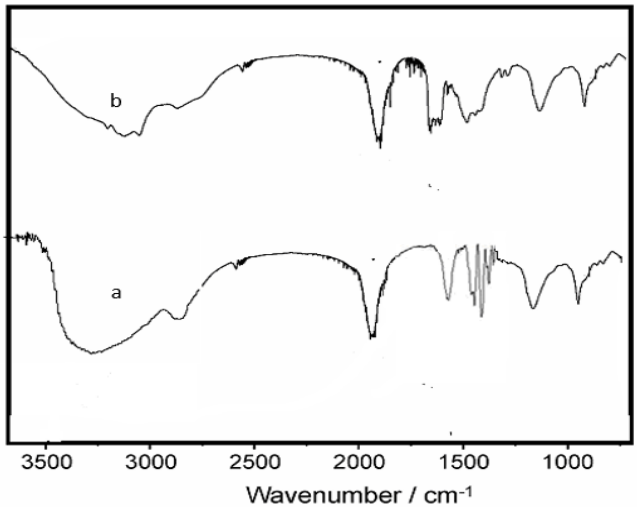

Figure 8: FTIR of of Bentonite/hematite /Acid res.

FTIR after 3 hrs shows a characterized broad peaks which assigned to the stretching OH band at 1153 cm^{-1}, the amine group peak at around 1495 cm^{-1} and the OH and NH peaks centered at 3420 cm^{-1}. After 24 hrs the FTIR shows an obvious difference in the intensity of amine group peak which can be related to interaction of these functional groups with the nano material [Chauhan A, Kaith B,2011]. The difference in intensity of this band between the spectrum at 3 hrs and this at 24 hrs of soaking suggested increasing in the interaction between both OH and amine groups in MO and the prepared nano magnetite by increasing the soaking time from 3 to 24 hrs.

Fig.8 a,b shows FTIR spectrum of Bentonite/hematite soaked in AR dye solution for 3 and 24 hrs respectively. The same bands are observed for OH and amine groups as in FTIR of MO loaded on nanoparticles. However here these two band have lower intensities and there are a noticed shift for OH and amine groups to higher wave numbers (3432 and 3445 cm^{-1}). This indicates the strong interaction between acid red dye and nano magnetite particles compared to those of MO dye. This confirms the removal efficiency results which showed higher removal of nanoparticles for AR than MO.

4 Conclusion

Bentonite coated with magnetic Fe_2O_3 can be used for the removal of anionic dyes from aqueous solutions. According to the obtained results both AR and CV showed maximum removal efficiency at pH 7 while MO at pH 4. The results showed there are high removal efficiency of the magnetic nanoparticles for the removal of the different organic dyes and the removal efficiency had the order CV > AR > MO. The results were related to the structure of the organic dye and the function groups on it. Acorrding to the results of FTIR there is a strong interaction between the function groups of the dye molecules and the magnetic nanoparticles. This interaction increase by increasing the contact time of the dye and the nanoparticles.

References

[1] Aksu Z. and Donmez G., A comparative study on the biosorption characteristics of some yeasts for Remazol Blue reactive dye, *Chemosphere*, **50**, 1075-1083, (2003).

[2] Baztias F.A. and Sidiras D.K., Dye adsorption by prehydrolysed beech sawdust in batch and fixed-bed systems, *Bioresour. Technol.* **98**, 1208-1217, (2006).

[3] Bhatnagar A. and Jain A.K., A comparative adsorption study with different industrial wastes as adsorbents for the removal of cationic dyes from water, *J. Colloid Interface Sci.* **281**, 49-55, (2005).

[4] Chauhan A, Kaith B, *Journal of Textile Science Engineering* **1**, 1–5, (2011).

[5] Chen S., Zhang J., Zhang C., Yue Q., Li Y.and Li E., Equilibrium and kinetic studies of methyl orange and methyl violet ad sorption on activated carbon derived from Phragmites australis, *Desalination*, **252**,149–150, (2010).

[6] Chung K.T., Fulk G.E. and Andrews, A.W., Mutagenicity

testing of some commonly used dyes, *Appl. Environ. Microbiol*, **42**, 641-648, (1981).

[7] Crini G, Non-conventional low-cost adsorbents for dye removal: a review, *Bioresour. Technol.* **97**, 1061-1085, (2006).

[8] Gupta V.K., Jain R., Varshney, S. and Saini, V.K., Removal of Reactofix Navy Blue 2 GFN from aqueous solutions using adsorption techniques, *J. Colloid Interface Sci.* **307**, 326-332, (2007).

[9] Gupta VK, Mittal A, Krishnan L, Gajbe V, Adsorption kinetics and column operations for the removal and recovery of malachite green from wastewater using bottom ash, *Sep. Purif. Technol.* **40**, 87–96, (2004).

[10] Herrea, F., Lopez, A., Mascolo, G., Albers, P., Kiwi, J. Catalytic combustion of orange II on hematite—surface species responsible for the degradation. *Appl. Catal. B: Environ.* **29**, 147–162, (2001).

[11] Jain, R. and Sikarwar S., Removal of hazardous dye congored from waste material, *J. Hazard. Mater*, 152, 942-948, (2008).

[12] Khattri S.D.and Singh M.K., Removal of malachite green from dye wastewater using neem sawdust by adsorption, *J. Hazard. Mater*, **67**, 1089-1094, (2009).

[13] Leechart P., Nakbanpote W. and Thiravetyan P., Application of 'waste' wood-shaving bottom ash for adsorption of azo reactive dye, *J. Environ. Manage.* **90**, 912-920, (2009).

[14] Li Y and Liu Y. , Removal of Pb(II) and Zn(II) from aqueous solution by ceramisite prepared by sintering bentonite, iron powder abd activated carbon, *Chem. Eng. J.*, **215-216**, 432-439, (2013).

[15] Liu Y, Kang Y, Mu B, Wang A, Attapulgite/bentonite interactions for methylene blue adsorption characteristics from aqueous solution, *Chem. Eng. J.* **237**, 403–410, (2014).

[16] Mittal A, Kurup L, Gupta VK, Use of waste materials—bottom ash and de-oiled soya, as potential adsorbents for the removal of Amaranth from aqueous solutions, *J. Hazard. Mater*, **117**, 171–176, (2005).

[17] Mittal A., Malviya A., Kaur D., Mittal J. and Kurup, L, Studies on the adsorption kinetics and isotherms for the removal and recovery of Methyl Orange from wastewaters using waste materials, **148**, 229-240, (2007).

[18] Naimeh A, Shadizadeh S. and Kazeminezhad I, Removal of Cadmium from drilling fluid using nanoadorbent, *fuel*, **111**, 505-509, (2013).

[19] Oliveira LCQ, Clay-iron oxide magnetic composites for the adsorption of contaminants in water. *Appl. Clay Sci.* **22**, 169-177, (2003).

[20] Tahir S, Rauf N, Removal of a cationic dye from aqueous solutions by adsorption onto bentonite clay, *Chemosphere* **63**, 1842–1848, (2006).